ELSEVIER

Journal of Photochemistry and Photobiology A: Chemistry 135 (2000) 1–5

Journal of Photochemistry and Photobiology A:Chemistry

www.elsevier.nl/locate/jphotochem

Photobleaching of the SO_2 $\tilde{C}^1B_2 \leftarrow \tilde{X}^1A_1$ transition caused by optically pumping the $\tilde{a}^3B_1$ state

Vladimir I. Makarov[1], Edwin Quiñones*

Department of Chemistry, University of Puerto Rico, P.O. Box 23346, San Juan, 00931-3346, Puerto Rico

Received 4 November 1999; received in revised form 3 February 2000; accepted 8 March 2000

Abstract

Fluorescence emerging from the $\tilde{C}^1B_2$ state of jet-cooled SO_2 was examined while pumping the $\tilde{a}^3B_1 \leftarrow \tilde{X}^1A_1$ transition, prior to exciting the $\tilde{C}^1B_2 \leftarrow \tilde{X}^1A_1$ transition. The $\tilde{C}^1B_2 \leftarrow \tilde{X}^1A_1$ transition is photobleached because the SO_2 molecules are 'shelved' in the triplet manifold, thereby reducing the occupation number of molecules in the ground state. The formation of $[SO_2]_n$ van der Waals (vdW) complexes significantly reduces the photobleaching of the 'hot' bands, which indicates that triplet SO_2 molecules are quenched within the environment of the clusters. In contrast, no significant changes in intensity is presented by the fundamental band possibly because the two-photon fragmentation of SO_2 into the O+SO fragments is taking place.

Keywords: Jet-cooled; Photobleaching; Transition

1. Introduction

The spectroscopy of SO_2 has been the subject of detailed studies [1–9]. Six electronic states of this molecule lie in the 9000–43 000 cm^{-1} spectral region, four of which can be reached optically from the ground $\tilde{X}^1A_1$ state: (a) $\tilde{a}^3B_1$ [1,12–16], (b) $\tilde{A}^1A_2$ [2–6,11], (c) $\tilde{B}^1B_1$ [2–6], and (d) $\tilde{C}^1B_2$ (τ_f=30–40 ns) [7–9]. An energy level diagram related to the present work is presented in Fig. 1. The collisionless lifetimes of the $\tilde{A}^1A_2$ and $\tilde{B}^1B_1$ states are strongly dependent on the excitation frequency [17–20]. The $^3B_2$ triplet state is metastable, whereas the $^3A_2$ triplet is optically unobservable [10,11].

In the present work, it was observed that the relative fluorescence intensities of the vibrational bands of jet-cooled SO_2, probed through the $\tilde{C}^1B_2 \leftarrow \tilde{X}^1A_1$ transition, show a strong laser fluence dependence. In part, this is because the main transition exhibits saturation effects, unlike the hot bands. Moreover, we find that the fluorescence intensity emerging from the $\tilde{C}^1B_2$ state decreases upon exciting the $\tilde{a}^3B_1 \leftarrow \tilde{X}^1A_1$ transition prior ($\Delta t \approx 100$ ns) to scanning the $\tilde{C}^1B_2 \leftarrow \tilde{X}^1A_1$ transition, and the spectra become 'cooler'. The experiment involved two separate measurements. First, laser induced fluorescence was observed from the $\tilde{C}^1B_2$ state, scanning the $\tilde{C}^1B_2 \rightarrow \tilde{X}^1A_1$ transition with a pulsed dye laser. The relative populations of different vibrational levels of the S_0 state can be extracted monitoring fluorescence from this transition. Second, the $\tilde{a}^3B_1 \leftarrow \tilde{X}^1A_1$ transition was excited prior to scanning the $\tilde{C}^1B_2 \leftarrow \tilde{X}^1A_1$ transition. Note that both transitions originate from S_0 and posses the following distinct characteristics: The $\tilde{C}^1B_2 \leftarrow \tilde{X}^1A_1$ transition is dipole-allowed and 'strong', whereas the $\tilde{a}^3B_1 \leftarrow \tilde{X}^1A_1$ transition is spin-forbidden and 'weak'. It follows that an intense light source was needed to optically populate the $\tilde{a}^3B_1$ state, and this was afforded employing the 355 nm output of a Nd:YAG laser. Even though in the absence of collisions the $\tilde{a}^3B_1$ state can undergo a number of intramolecular processes (see Fig. 1), none of them places population back into S_0. In other words, with respect to the time scale of the present experiments, triplet SO_2 molecules may be regarded as being 'shelved' in the triplet manifold. The reduction in the occupation number of molecules in S_0 associated to the excitation to the triplet manifold was monitored by measuring the depletion in fluorescence intensity (or photobleaching). On the other hand, the recovery of the fluorescence signal was observed working under conditions at which $[SO_2]_n$ van der Waals clusters (vdW) are formed. This observation provided circumstantial evidence

* Corresponding author.

[1] Present address: Institute of Chemical Kinetics and Combustion, 630090 Novosibirsk, Russian Federation.

1010-6030/00/$ – see front matter
PII: S1010-6030(00)00269-0

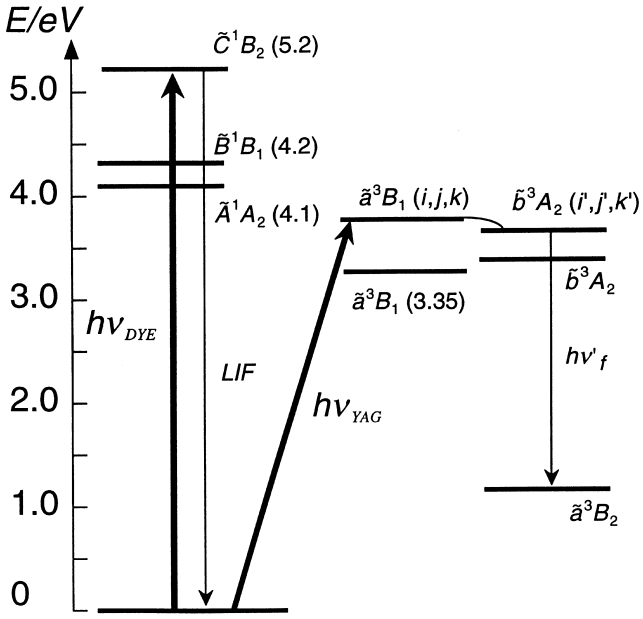

Fig. 1. Diagram of the electronic states of the SO_2 molecule relevant to the present work. The $\tilde{C}^1B_2 \leftarrow \tilde{X}^1A_1$ transition was examined monitoring fluorescence. In some experiment the $\tilde{a}^3B_1 \leftarrow \tilde{X}^1A_1$ transition was excited using the 355 nm output of a Nd:YAG laser, prior to exciting the singlet transition.

suggesting that triplet SO_2 molecules are undergoing electronic deactivation to the ground state within the 'cage' of the $[SO_2]_n$ vdW clusters.

Similar photochemical processes in clusters have attracted considerable attention in recent years [21–27]. The dissociation and cage recombination of I_2 molecules under cluster conditions has been presented by Roncero et al. [28]. Studies of the $I_2(Ar_n)$ clusters [29–31] have provided a detailed microscopic picture of the caging effect. The concept of the solvent cage has been extended to explain why the predissociation of diatomic molecules such as OH and SH is blocked when the OH–Ar and SH–Ar vdW clusters are formed [32].

2. Experimental

2.1. Description of the apparatus

The molecular beam apparatus employed in the present experiments has been described elsewhere [33]. A pulsed electromagnet valve (General Valve Series 9) with a 0.8 mm nozzle diameter was used to rotationally cool the SO_2 molecule and to form $[SO_2]_n$ van der Waals clusters. The fluorescence signal from the expanded Ar/SO_2 mixtures was observed 25 nozzle diameters down stream. The background pressure in the chamber prior to operating the pulsed valve was about 10^{-6} Torr. The third harmonic (λ_{ex}=355 nm) of a Nd:YAG laser (Continuum Surelite II) was utilized to pump the $\tilde{a}^3B_1 \leftarrow \tilde{X}^1A_1$ transition of SO_2. Laser pulses of 3 mJ were focused onto on area of 1 mm^2 using a lens (f=100 cm). An excimer pumped-dye laser (Λ-Physik LPD 3002) equipped with a BBOI doubling crystal allowed the scan of the laser excitation spectra. Coumarin-47 was the dye employed. The dye laser beam was colinearly counter propagated to that of the Nd:YAG laser. A time delay of 100 ns between the lasers pulses was controlled by a digital delay pulse generator (Stanford Research DG535). The laser induced fluorescence was recorded by a frontal photomultiplier (Thorn EMI) and the signal was integrated by a boxcar (Stanford Research SR 250). The data acquisition was performed by a personal computer (Macintosh IIci) linked to the boxcar integrator and other devices through a GW interface (GW Instrument MacAdios II card), programmed with MPW FORTRAN. Each data point was averaged for five laser pulses. The dye laser pulse energy was measured at every wavelength using a pyroelectric joulemeter (Molectron Mod. J3), and the signal was fed into the computer to correct the spectra. The spectral resolution was 0.1–0.2 cm^{-1}.

Commercial SO_2 (Air Products) was used without further purification. The SO_2 samples were diluted in Ar to a 3–5%. The total pressure above the pulsed valve was varied in the 0.5–6.0 bar range.

2.2. Spectroscopic simulations

The position of the SO_2 vibrational bands in the $\tilde{C}^1B_2 \leftarrow \tilde{X}^1A_1$ laser fluorescence excitation spectra were assigned using a computer simulation. To this end, the following equation was used:

$$\omega_{\tilde{C}\leftarrow\tilde{X}} = \omega_{0-0} - n_1''\nu_1'' - n_2''\nu_2'' - n_3''\nu_3'' + n_1'\nu_1' + n_2'\nu_2' + n_3'\nu_3' \quad (1)$$

where n_i'' and ν_i'' denote the vibrational quantum numbers and vibrational frequencies of the vibrational modes of SO_2 in the ground state, n_i' and ν_i' are the vibrational quantum numbers and vibrational frequencies of the vibrational modes of the SO_2 $\tilde{C}^1B_2$ state, and ω_{0-0}=42 625.75 cm^{-1}. For the ground state, the values for ν_1', ν_2', ν_3' are 1151.38, 517.69 and 1361.76 cm^{-1}, respectively, while ν_1'', ν_2'', ν_3'' for state $\tilde{C}^1B_2$ are 963, 377 and 284 cm^{-1}, respectively [1–16].

3. Results and discussion

3.1. Laser fluence dependence of the SO_2 $\tilde{C}^1B_2 \leftarrow \tilde{X}^1A_1$ transition

Fig. 2(a) displays a laser fluorescence excitation spectrum of the SO_2 on the $\tilde{C}^1B_2 \leftarrow \tilde{X}^1A_1$ transition in the 234.5–237.0 nm region. A 5% SO_2/Ar mixture was expanded in a supersonic free jet at a backing pressure of 4 bar. To simulate the spectrum shown in Fig. 2(a) it is sufficient to include the (0,0,0), (0,1,0) and (0,2,0) vibrational levels in the ground state. The most intense band,

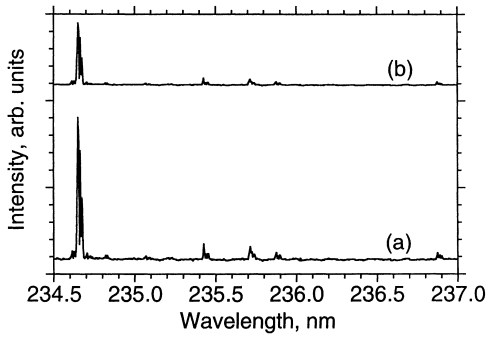

Fig. 2. (a) Laser fluorescence excitation spectrum of SO_2 on the $\tilde{C}^1B_2 \leftarrow \tilde{X}^1A_1$ transition. A 5% SO_2/Ar mixture was expanded in a supersonic free jet at a backing pressure of 4 bar. (b) The $\tilde{a}^3B_1 \leftarrow \tilde{X}^1A_1$ transition was excited a 100 ns prior to exciting the $\tilde{C}^1B_2 \leftarrow \tilde{X}^1A_1$ transition. In both spectra the laser pulse energy was low to avoid optical saturation and non-linear processes.

centered around 234.6 nm (5.28 eV), corresponds to the $\tilde{C}^1B_2(0,0,0) \leftarrow \tilde{X}^1A_1(0,0,0)$ transition (from now on denoted the fundamental band). The rest of the bands in the spectrum are 'hot' bands. Fig. 1 displays the relative position of the $\tilde{C}^1B_2$ and $\tilde{X}^1A_1$ states along with other electronic states relevant to the present work. The laser fluence dependence of the $\tilde{C}^1B_2(0,0,0) \leftarrow \tilde{X}^1A_1(0,0,0)$ transition was studied monitoring fluorescence intensity at the maximum of the band. It is noted from Fig. 3 that the fluorescence intensity from this band increases linearly with laser pulse energy, reaches a plato, and then decreases to half of its maximum intensity. In contrast, the fluorescence intensity from the $\tilde{C}^1B_2(0,0,1) \leftarrow \tilde{X}^1A_1(0,1,0)$ 'hot' band exhibits a linear behavior in the same laser fluence range.

The non-linear behavior displayed by the fluorescence intensity from the $\tilde{C}^1B_2$ state fundamental band against dye laser fluence is consistent with the occurrence of multiphoton processes. Accordingly, we identified other molecular processes that could become important at high laser fluences. Specifically, the SO_2 photodissociation and ionization thresholds are at 5.64 eV (220 nm) and 12.34 eV,

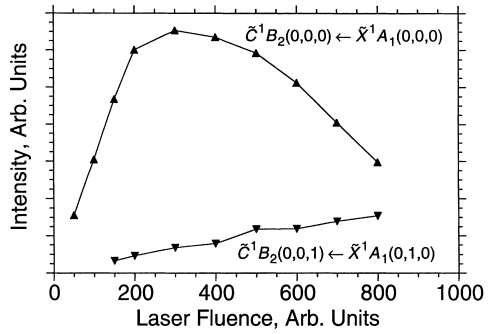

Fig. 3. (a) Fluorescence intensity from the $\tilde{C}^1B_2(0,0,0) \leftarrow \tilde{X}^1A_1(0,0,0)$ fundamental band, which increases linearly as the laser pulse energy is increased, reaches a plato, and then decreases, (b) the fluorescence intensity from the $\tilde{C}^1B_2(0,0,1) \leftarrow \tilde{X}^1A_1(0,1,0)$ 'hot' band exhibits a linear behavior in the same laser fluence range.

respectively. The $\tilde{C}^1B_2(0,0,0) \leftarrow \tilde{X}^1A_1(0,0,0)$ transition (5.28 eV) lies below those limits. On the other hand, the two-photon absorption of SO_2 at 234.6 nm (10.6 eV), $SO_2 + 2h\nu \rightarrow O + SO$, is above the dissociation limit, but below the ionization threshold. The SO_2 ionization at 234.6 nm would require the absorption of three photons (15.85 eV): $SO_2 + 3h\nu \rightarrow SO_2^+ + e^-$. Considering that we are exciting with a dye laser with relatively low energy per pulse (0–2.7 mJ per pulse), the two-photon dissociation process seems to be the most probable one.

3.2. Optical reduction of the SO_2 occupation number in the ground state

If the $\tilde{a}^3B_1 \leftarrow \tilde{X}^1A_1$ transition is pumped at 355 nm (3.49 eV) 100 ns prior to exciting the $\tilde{C}^1B_2 \leftarrow \tilde{X}^1A_1$ transition, the fluorescence intensity from the fundamental band as well as that of the 'hot' bands decreases a 50%, as Fig. 2(b) depicts. The spectra displayed in Fig. 2 were collected at a laser fluence well below the non-linear region exhibited by the fundamental band. The fluorescence intensity emanating from the $\tilde{C}^1B_2$ state is reduced because the Nd:YAG laser populates $\tilde{a}^3B_1(\upsilon_1, \upsilon_2, \upsilon_3)$ levels from the ground state. This experiment provides indirect evidence that we are pumping the $\tilde{a}^3B_1 \leftarrow \tilde{X}^1A_1$ transition with the third harmonic of the Nd:YAG laser, as the $\tilde{C}^1B_2 \leftarrow \tilde{X}^1A_1$ transition also originates from the ground state.

3.3. Transitions in the triplet manifold

The 355 nm output of the Nd:YAG laser can excite the $\tilde{a}^3B_1(0,2,0)$ triplet state, as Fig. 1 schematically shows. For numerical analysis, Eq. (1) was also applied, employing the corresponding frequencies for the $\tilde{a}^3B_1$ state [1,12–16]. It has been shown [1] that triplet state levels lying above the $\tilde{a}^3B_1(0,2,0)$ level are strongly perturbed by intramolecular interactions (e.g. electronic-vibrational, spin-orbit) induced by the neighboring levels of the $^3A_2$ triplet. Thus, intramolecular transitions can occur between vibrationally excited levels of the $\tilde{a}^3B_1$ state and levels of the state. Moreover, transitions between the $^3A_2$ and $^3B_2$ the state are electric dipole allowed [34–38]. However, the ground state is not populated back by any of such transitions or processes and the triplet SO_2 molecules are 'shelved' in the triplet manifold.

3.4. Clustering effects

Fig. 4(a) shows a laser excitation spectrum of SO_2 in the same spectral region examined in Fig. 1, but scanning the dye laser at the maximum fluence reached in Fig. 3. At this laser fluence, the main transition is being saturated and we believe the SO_2 photodissociation is taking place. These spectra were collected expanding a 3% SO_2/Ar mixture from a stagnation pressure of 480 Torr into the vacuum chamber.

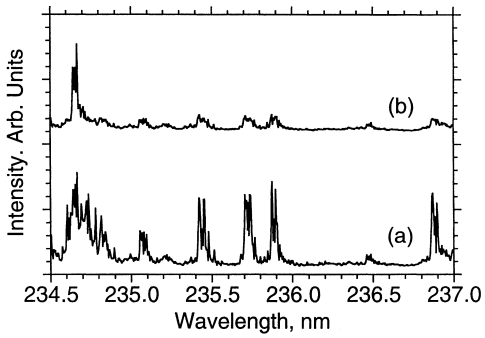

Fig. 4. (a) Laser fluorescence excitation spectrum of jet cooled SO_2 on the $\tilde{C}^1B_2 \leftarrow \tilde{X}^1A_1$ transition. A 3% SO_2/Ar mixture was expanded in a supersonic free jet at a backing pressure of 480 Torr. (b) The $\tilde{a}^3B_1 \leftarrow \tilde{X}^1A_1$ transition was excited a 100 ns prior to exciting the $\tilde{C}^1B_2 \leftarrow \tilde{X}^1A_1$ transition. In both spectra the dye laser fluence was the highest shown in Fig. 3. At this dye laser fluence the $\tilde{C}^1B_2(0,0,0) \leftarrow \tilde{X}^1A_1(0,0,0)$ transition is saturated, although the 'hot' bands are not.

Rotational cooling is achieved working at this low stagnation pressure, while SO_2 clustering is minimized. The fluorescence intensity from the 'hot' bands decreases to a 15% when the Nd:YAG laser is driving the $\tilde{a}^3B_1 \leftarrow \tilde{X}^1A_1$ transition, as Fig. 4(b) shows. This clearly reflects a decrease in the population of ground state molecules.

A much cooler spectrum is obtained upon increasing the stagnation pressure to 6 bar, as Fig. 5(a) shows. These strong expansion conditions favor the formation of $[SO_2]_n$ vdW clusters. Moreover, in this experiment the dye laser output is high (the same used in Fig. 4), which means that the main band exhibits non-linear behavior. A reduction to only a 50% in the fluorescence intensity of the 'hot' bands is observed when the Nd:YAG laser is pumping the $\tilde{a}^3B_1 \leftarrow \tilde{X}^1A_1$ transition, as displayed in Fig. 5(b). The same experiment was performed at backing pressures of 1.7 and 4 bar and a gradual increase in the relative fluorescence was

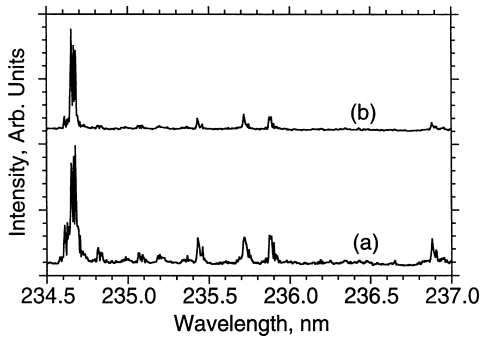

Fig. 5. (a) Laser fluorescence excitation spectrum of SO_2 on the $\tilde{C}^1B_2 \leftarrow \tilde{X}^1A_1$ transition. A 3% SO_2/Ar mixture was expanded in a supersonic free jet at a backing pressure of 6 bar. (b) The $\tilde{a}^3B_1 \leftarrow \tilde{X}^1A_1$ transition was excited a 100 ns prior to scanning the $\tilde{C}^1B_2 \leftarrow \tilde{X}^1A_1$ transition. In both spectra the dye laser fluence was the highest shown in Fig. 3. At this dye laser fluence the $\tilde{C}^1B_2(0,0,0) \leftarrow \tilde{X}^1A_1(0,0,0)$ transition is saturated, although the 'hot' bands are not. At the backing pressure employed in this experiment the SO_2 molecules excited to the triplet manifold are relaxed within the environment of the $[SO_2]_n$ clusters.

also observed (data not shown). This means that a larger number of SO_2 molecules are clustered upon increasing the backing pressure, thereby enhancing the probability of relaxation of triplet molecules. In contrast, the intensity of the fundamental band does not change significantly because this band is being observed in the non-linear region and at this laser fluence only a small fraction of the molecules end up being excited to the $\tilde{C}^1B_2$ state. In fact, the fluorescence intensity that one should expect can be estimated extrapolating the initial slope in Fig. 3 (the first four points in the curve for the 0–0 transition) to the highest laser fluence. Clearly, the SO_2 molecules are undergoing a photochemical process, one of which could be two-photon photodissociation.

The reduction observed on the magnitude of the photobleaching of the 'hot' bands as the backing pressure is increased may be explained as follows. At the higher backing pressures triplet SO_2 molecules undergo electronic relaxation to S_0 in the environment of the clusters. This happens before the probe laser pulse excites the $\tilde{C}^1B_2 \leftarrow \tilde{X}^1A_1$ transition. In other words, since the fluorescence intensity from the 'hot' bands as a function of backing pressure converges towards the value when the Nd:YAG laser beam is turned off we can conclude that there is triplet relaxation within the cluster environment. Note that the linear behavior exhibited by the 'hot' bands as a function of laser fluence indicates that we are exciting the electronic transition without inducing other processes.

One can anticipate that the 'cage' effect due to the formation of $[SO_2]_n$ vdW clusters should favor the $O+SO \rightarrow SO_2$ recombination process, if this is happening when we excite the fundamental band at the higher laser pulse energies. However, changes in the intensity of the fundamental band are not observed upon increasing the backing pressure (to favor the formation of $[SO_2]_n$ vdW clusters) and we do not have evidence to argue that the recombination is taking place. This may be because the available energy (5.0 eV) to be distributed between the O+SO fragments, formed from the two-photon dissociation process, is much larger than the energy required for the fragmentation of the $[SO_2]_n$ vdW clusters. Thus, the SO_2 clustering seems to be effective to relax the $\tilde{C}^1B_2$ state, but not to recombine the O+SO fragments to form the S_0 state.

4. Concluding remarks

Marked changes are observed in the $\tilde{C}^1B_2 \leftarrow \tilde{X}^1A_1$ laser fluorescence excitation spectra if the $\tilde{a}^3B_1 \leftarrow \tilde{X}^1A_1$ transition is pumped using the third harmonic of the Nd:YAG laser, prior to exciting the $\tilde{C}^1B_2$ state. This effect is due to the trapping of the SO_2 molecules in the triplet manifold. The SO_2 molecules excited to the triplet state return to the ground state when triplet SO_2 molecules are embedded in the $[SO_2]_n$ clusters. Clustering effects do not appreciably affect the behavior of the SO_2 fundamental band when the probe laser fluence is high. This may be attributed to the

two-photon dissociation of the SO_2 molecule, but this result was not experimentally confirmed.

Acknowledgements

The financial support for this work from the US Department of Energy EPSCoR Program is gratefully acknowledged. The excimer laser was purchased with funds of the Puerto Rico Laser Facility, under the auspices of the RCMI Program and NSF-EPSCoR.

References

[1] J.C.D. Brand, C. di Lauro, V.T. Jones, J. Mol. Spectrosc. 45 (1973) 404.
[2] Y. Hamada, A.J. Merer, Can. J. Phys. 52 (1974) 1443.
[3] A. Fischer, R. Kulmer, W. Demtroder, Chem. Phys. 83 (1984) 415.
[4] R. Kulmer, W. Demtroder, J. Chem. Phys. 81 (1984) 2919.
[5] R. Kulmer, W. Demtroder, Chem. Phys. 92 (1985) 423.
[6] K. Kulmer, W. Demtroder, J. Chem. Phys. 83 (1985) 2712.
[7] W. Sharfin, M. Ivanko, S.C. Wallace, J. Chem. Phys. 76 (1982) 2095.
[8] R.H. Dixon, M. Halle, Chem. Phys. Lett. 22 (1973) 450.
[9] J.C.D. Brand, K. Srikameswaran, Chem. Phys. Lett. 15 (1972) 130.
[10] I.H. Hiller, V.R. Saunders, Mol. Phys. 22 (1971) 193.
[11] J.C.D. Brand, J.L. Hardwick, D.R. Humphrey, Y. Hamada, A.J. Merer, Can. J. Phys. 54 (1976) 186.
[12] A.J. Merer, Dis. Faraday Soc. 35 (1963) 127.
[13] H.D. Mettee, J. Chem. Phys. 49 (1968) 1784.
[14] J.C.D. Brand, C. di Lauro, V.T. Jones, J. Am. Chem. Soc. 92 (1970) 6095.
[15] J.C.D. Brand, V.T. Jones, C. di Lauro, J. Mol. Spectrosc. 40 (1971) 616.
[16] J.P. Vikesland, S.J. Strickler, J. Chem. Phys. 60 (1974) 660.
[17] E. Brus, J.R. McDonald, J. Chem. Phys. 61 (1974) 97.
[18] F. Su, N.W. Bottenheim, H.W. Sidebottom, J.G. Calvert, E.K. Damon, Int. J. Chem. Kinet. 10 (1978) 125.
[19] D.L. Holtermann, E.K.C. Lee, J. Chem. Phys. 77 (1982) 5327.
[20] R. Kulmer, W. Demtroder, J. Chem. Phys. 84 (1986) 3672.
[21] S.K. Shin, Y. Chen, S. Nickolaisen, S.W. Sharpe, R.A. Beaudet, C. Wittig, Adv. Photochem. 16 (1991) 248.
[22] A.W. Castleman Jr., S. Wei, Annu. Rev. Phys. Chem. 45 (1994) 685.
[23] R.B. Gerber, A.B. McCoy, A. Garcia-Vela, Annu. Rev. Phys. Chem. 45 (1994) 275.
[24] E.R. Bernstein, Annu. Rev. Phys. Chem. 46 (1995) 197.
[25] K. Bergmann, J.R. Huber, J. Phys. Chem. 101 (1997) 259.
[26] J.K. Wang, Q. Liu, A.H. Zewail, J. Phys. Chem. 99 (1995) 11309.
[27] Q. Liu, J.K. Wang, A.H. Zewail, J. Phys. Chem. 99 (1995) 11321.
[28] P. Roncero, N. Halberstadt, J.A. Beswick, in: J. Jortner (Ed.), Reaction Dynamics in Clusters and Condensed Phases, Kluwer Academic Publishers, Netherlands, 1994, p. 73.
[29] E.D. Potter, Q. Liu, A.H. Zewail, Chem. Phys. Lett. 200 (1992) 605.
[30] Q. Liu, J.K. Wang, A.H. Zewail, Nature 364 (1993) 427.
[31] J.M. Papanikolas, J.R. Gord, N.E. Levinger, D. Ray, V. Vorsa, W.C. Lineberger, J. Phys. Chem. 95 (1991) 8028.
[32] E.R. Bernstein (Ed.), Chemical Reactions in Clusters, Oxford University Press, New York, 1996.
[33] C. Conde, C. Maul, E. Quiñones, J. Phys. Chem. A 103 (1999) 1929.
[34] F. Su, F.B. Wampler, J.W. Bottenheim, D.L. Thorsell, J.G. Calvert, E.K. Damon, Chem. Phys. Lett. 51 (1977) 150.
[35] F.B. Wampler, R.C. Oldenborg, W.W. Rice, R.R. Karl, J. Chem. Phys. 69 (1978) 2569.
[36] S.J. Strickler, R.N. Rudolph, J. Am. Chem. Soc. 100 (1978) 3326.
[37] F.B. Wampler, R.C. Oldenborg, W.W. Rice, Int. J. Chem. Kinet. 11 (1979) 125.
[38] S.J. Strickler, R.D. Ito, J. Phys. Chem. 89 (1985) 2366.